Contribution No. 3830 from the Department of Chemistry, University of California, Los Angeles, California 90024

Ligand Substitution Photochemistry of Monosubstituted Derivatives of Tungsten Hexacarbonyl

R. MARC DAHLGREN and JEFFREY I. ZINK*

Received May 12, 1977 AIC70344N

The photosubstitution chemistry of the compounds $W(CO)_5L$ (L = acetonitrile, NH_3, cyclohexylamine, pyridine, piperidine, PPh_3, PBr_3, PCl_3, PH_3, $P(n\text{-}Bu)_3$, CS, Br^-, methylmethoxycarbene, and phenylmethoxycarbene) follows three categories of photoreactivity. Nitrogen-donor complexes show efficient unique ligand photosubstitution with reduced carbon monoxide replacement. Phosphorus-donor materials undergo both efficient carbon monoxide and unique ligand substitution. The remaining compounds show reduced substitution efficiency in all metal–ligand bond types. A mechanism for the photosubstitution is proposed. The mode of the ligand substitution reaction path is interpreted in terms of a ligand inductive effect which is manifest in the carbon–oxygen bond order. The magnitude of the quantum yields is a consequence of either the relative bond weakening in the excited state or enhanced nonradiative deactivation from this state.

Introduction

The group 6B metal carbonyls and their derivatives have been the subject of photochemical investigation since the observation of the photosensitivity of the parent hexacarbonyls in 1961.[1] Initially, great advantage was taken of the high quantum efficiency and stereospecificity of the photochemical substitution reactivity of these compounds in the synthesis of novel and thermally inaccessible materials.[2] The utility of these photoreactions has been expanded through quantitative studies.[3,4] Studies of $W(CO)_5(py)$[5,6] have shown that pyridine photosubstitution is highly efficient but carbon monoxide replacement occurs at a much reduced rate. A variety of tungsten pentacarbonylammine complexes have been investigated.[7] Again unique ligand photosubstitution dominates when the lowest excited state is populated. When a charge-transfer state becomes lowest in energy as is the case for many substituted pyridine complexes of the type $W(CO)_5L$, all ligand substitution processes proceed at reduced quantum efficiency.[8]

Until now, systematic, quantitative investigation of the effect of a diverse array of unique ligands on the photochemistry of $W(CO)_5L$ compounds has not been undertaken. These materials are very attractive systems for study owing to their relative ease of preparation, simple identification of photoproducts with infrared spectroscopy,[9] and convenient molecular orbital and ligand field theoretical treatments arising from the high C_{4v} microsymmetry and small number of atoms in the complexes. The tungsten complexes were chosen over the chromium or molybdenum materials because of their high thermal and atmospheric stability. The motivation underlying this study has been to elucidate those aspects of the lowest energy excited state of the monosubstituted derivatives of tungsten hexacarbonyl which influence the efficiency and the mode of ligand photosubstitution.

The bonding properties of the unique ligand, L, in these $W(CO)_5L$ complexes perturb the nature of the lowest excited state and as such give rise to a mechanism by which this state may be fine tuned to provide a variety of photochemical consequences. Variation of L leads to three contrasting modes of photosubstitution reactivity. The metal–ligand bonds which are photolabilized may be correlated with the inductive and mesomeric properties of L. The relative efficiency of these processes is explainable from either changes in the rate of nonradiative deactivation processes or the magnitude of net metal–ligand bond order changes in the excited state. Mechanistic aspects of the overall photoreactions are determined by varying the conditions under which the primary photointermediates are scavenged. Thus, this quantitative investigation of a wide variety of $W(CO)_5L$ complexes enables the formulation of a theoretical model which embodies those excited state characteristics most influencing the photochemical reaction pathway in highly covalent materials.

Experimental Section

1. Preparation and Characterization of Compounds. The monosubstituted derivatives of tungsten hexacarbonyl, with the exceptions described below, were prepared by standard techniques. Tungsten hexacarbonyl was obtained from Strem Chemicals and used without further purification. All solvents were reagent grade and handled as described in the literature preparations. Reactions were carried out under a blanket of prepurified nitrogen. With the exception of PH_3, CS, and the carbenes, the unique ligands are all common reagents and were used without purification. Organolithium reagents were obtained from Alfa. Thiophosgene and "magic methyl" were purchased from Aldrich.

$W(CO)_5(AN)$[10] (AN = acetonitrile), $W(CO)_5NH_3$, $W(CO)_5(c\text{-}HxNH_2)$,[11] $W(CO)_5P(n\text{-}Bu)_3$, $W(CO)_5(pip)$,[12] and $W(CO)_5(py)$[11] were prepared by photolysis of tungsten hexacarbonyl in an Ace photochemical immersion well with a 550 W Hanovia UV Source. All IR spectra were run in cyclohexane.

$W(CO)_5(AN)$.[10] Reported[13] carbonyl IR (cm^{-1}): 2038, 1948, 1931. Found: 2077, 1944, 1926. Melting point: 82 °C dec.

$W(CO)_5NH_3$. $W(CO)_6$ (1.36 g) was irradiated in 100 mL of THF for 2 h with constant N_2 purge. After photolysis, anhydrous NH_3 gas was passed through the yellow solution producing a yellow precipitate which was collected by filtration. Sublimation at 50 °C (1 mm) for several hours removed residual $W(CO)_6$. The yellow residue was twice recrystallized from 1:1 (v/v) hexane–ether. Anal. Calcd for $WC_5O_5NH_3$: C, 17.60; H, 0.89. Found: C, 18.00; H, 0.99.

$W(CO)_5(c\text{-}HxNH_2)$.[11] Anal. Calcd for $WC_{11}O_5NH_{13}$: C, 31.22; H, 3.10. Found: C, 32.01; H, 3.29. Reported[12] carbonyl IR (cm^{-1}): 2072, 1931.5, 1918.5. Found: 2072, 1930, 1917. Melting point: 120–122 °C.

$W(CO)_5P(n\text{-}Bu)_3$. $W(CO)_6$ (2.00 g) and 5.0 mL of *n*-butylphosphine were irradiated in 50 mL of THF for 2 h under N_2 purge. This solution was rotovaped to dryness and the brown residue was extracted with pentane and twice chromatographed on alumina with pentane elution. The yellow band was isolated and the pentane was removed at 20 °C under high vacuum over 24 h resulting in a yellow viscous oil. Reported[14] carbonyl IR (cm^{-1}): 2068.5, 1943, 1935.5. Found: 2065, 1941, 1935.

$W(CO)_5(pip)$.[12] Reported[12] carbonyl IR (cm^{-1}): 2073, 1928, 1918. Found: 2065, 1926, 1917. Melting point: 110–115 °C dec.

$W(CO)_5(py)$.[11] Anal. Calcd for $WC_{10}O_5NH_5$: C, 29.80; H, 1.25. Found: C, 27.18; H, 1.67. Reported[11] carbonyl IR (cm^{-1}): 2073.0, 1935.0, 1921.0. Found: 2072, 1932, 1919.

$W(CO)_5Br^-NEt_4^+$[15] and **$W(CO)_5PPh_3$**[16] were prepared by the thermal reaction of the ligand with $W(CO)_6$.

$W(CO)_5Br^-NEt_4^+$.[15] Anal. Calcd for $WC_{13}O_5H_{20}NBr$: C, 29.23; H, 3.78. Found: C, 29.44; H, 3.93. Carbonyl IR in KBr disk (cm^{-1}): 2072, 1923, 1893.

$W(CO)_5PPh_3$.[16] Anal. Calcd for $WC_{23}O_5PH_{15}$: C, 47.12; H, 2.58; P, 5.28. Found: C, 47.69; H, 2.84; P, 5.45. Reported[14] carbonyl

IR (cm^{-1}): 2075, 1944. Found: 2072, 1944. Reported[16] melting point: 146 °C. Found: 142 °C.

(Ac)W(CO)$_5^-$NMe$_4^+$.[17] Anal. Calcd for $WC_{11}O_6NH_{15}$: C, 29.95; H, 3.43. Found: C, 28.21; H, 3.49.

(Bz)W(CO)$_5^-$NMe$_4^+$.[17] Anal. Calcd for $WC_{16}O_6NH_{17}$: C, 38.19; H, 3.41. Found: C, 37.83; H, 3.51.

W(CO)$_5$(methylmethoxycarbene). (Ac)$W(CO)_5^-NMe_4^+$ (0.22 g) was suspended in 50 mL of Et_2O in a Schlenck apparatus under N_2 with constant stirring. FSO_3CH_3 (0.5 mL), "magic methyl", was added with a syringe producing a white precipitate and a yellow solution. The precipitate was removed by filtration under N_2. The solvent was then removed in vacuo and the resulting yellow residue was sublimed at 45–50 °C (1 mm) forming large yellow air-stable crystals. Reported (Nujol)[17] carbonyl IR (cm^{-1}): 2083, 1988, 1946. Found (cyclohexane): 2075, 1961, 1938.

W(CO)$_5$(phenylmethoxycarbene) was prepared in the same fashion as the methylmethoxycarbene using 0.50 g of (Bz)$W(CO)_5^-NMe_4^+$, 100 mL of Et_2O, and 1.0 mL of FSO_3CH_3 resulting in red air-stable needles. Reported (Nujol)[17] carbonyl IR (cm^{-1}): 2079, 1992, 1953. Found (cyclohexane): 2073, 1961, 1944. ^1H NMR: 2.56 ppm (τ phenyl), 8.53 ppm (τ CH_3).

W(CO)$_5$PBr$_3$.[18] Reported[19] carbonyl IR (cm^{-1}): 2093, 1991, 1982. Found: 2095, 1990, 1984.

W(CO)$_5$PCl$_3$ was prepared in the same manner as the PBr_3 complex.[18] Reported[19] carbonyl IR (cm^{-1}): 2095, 1990, 1984. Found: 2083, 1985, 1981.

W(CO)$_5$PH$_3$ was prepared in analogy to ref 20 from $W(CO)_5Br^-NEt_4^+$. PH_3 was generated from AlP_4 with HCl. Carbonyl IR (cm^{-1}): 2095, 1956. Reported[21] ^1H NMR: (τ PH_3) 7.49 ppm ($^1J_{^{31}P-^1H}$ = 341 Hz, C_6D_6). Found: (τ PH_3) 7.46 ppm ($^1J_{^{31}P-^1H}$ = 345 Hz, C_6D_6).

W(CO)$_5$CS.[22] Repeated crystallization from pentane was used to purify the material. After five recrystallizations the substance was judged to contain less than 1.5% $W(CO)_6$ as an impurity based on the carbonyl IR spectrum. Reported[22] carbonyl IR (cm^{-1}): 2096, 2007, 1989. Found: 2097, 2008, 1989.

2. Quantum Yield Determinations. Solvents used for quantitative photolysis were purified before use as described by Jolly.[23] Cyclohexane was purified using the method described for *n*-hexane. All distillations were performed under nitrogen. Because pure $CHCl_3$ caused decomposition of the complexes during photolysis, 0.75% absolute ethanol was added to the purified solvent as a stabilizer.

All quantum yields were determined on an optical bench using monochromatic light achieved by chemical filtering. Actinometry was done with the $K_3Fe(C_2O_4)_3$ system described in Calvert and Pitts.[24a] Light at 4358 Å was isolated from the output of a PEK-110, 100-W high-pressure Hg source using the standard $NaNO_2$, $CuSO_4/NH_4OH$ chemical filter combination.[24b] The maximum band-pass was ±50 Å as measured by passing the beam through a 0.25-m monochromator. The average photon flux at this wavelength was approximately 8.5×10^{15} photons/s over the face of the cells. Samples were irradiated in 10-cm Cary-type quartz cells of 25-mL capacity held in a thermostated brass block maintained at 7 °C. The 4050-Å Hg line was isolated from a Hanovia 1000-W Hg source. The beam was coalesced with Pyrex lenses and traveled through a 5 cm recirculating water filter, a 1 cm saturated aqueous $NaNO_2$ solution, a Corning 7-51 glass filter, and a 29-4 5000 Å cut-off filter to produce a monochromatic beam centered at 4050 ± 100 Å. The average light intensity was approximately 1.0×10^{15} photons/s over the cell face. Samples were contained in 1-cm Beckman-type quartz cells (non-thermostated) resting on a magnetic stirrer and fitted with a "micro" stirring bar. The concentration of $W(CO)_5L$ was chosen to cause at least 75% absorption of the incident light (i.e., about 2×10^{-2} M for phosphine complexes at 4050 Å (1 cm), 2×10^{-4} M for amine materials at 4358 Å (10 cm), and 5×10^{-4} for the other complexes at 4050 Å (1 cm)).

For those systems in which isosbestic points were found, product identification and fractional conversion, f, were determined from UV–visible spectral analyses using eq 1 at several wavelengths. A_λ

$$A_\lambda = \{(1-f)W_0\epsilon_{st} + fW_0\epsilon_{pp}\}l \quad (1)$$

is the optical density of a sample of path length l at wavelength λ, W_0 is the total concentration of tungsten in the system, and ϵ_{st} and ϵ_{pp} are the molar absorptivities of the starting material and the photoproduct, respectively. f was averaged for the several wavelengths examined to arrive at the fraction photochemically converted to product. When no isosbestic points occurred, the relative concentration and identity of the various compounds were calculated from the integrated intensity of their corresponding carbonyl infrared bands. In these cases (i.e., $W(CO)_5PR_3$ compounds with CO entering ligand) Beer's law plots of the integrated intensity of the T_{1u} $W(CO)_6$ vibration were used to establish the appearance quantum yield. No significant difference in this appearance quantum yield and that for disappearance of $W(CO)_5L$, based on the $A_1^{(1)}$ vibrational band, could be found for short irradiation periods. The infrared instrument was calibrated with neutral density filters before each run. After photolysis, the samples were transferred in the dark to analysis cells under atmospheric conditions. Between the time of photolysis and analysis all samples were frozen at −80 °C in the dark in sealed tubes under N_2.

The quantum yields were calculated using an iterative least-squares fit of the concentration–irradiation time data with a theoretical disappearance curve which accounts for the effect of inner-filtering in the samples. For a reaction in which species A is converted to B, the rate of disappearance of A is defined by eq 2 where Φ is the

$$-\frac{d[A]}{dt} = \frac{\Phi I_0}{NV}\frac{\epsilon_A[A]}{\epsilon_A[A]+\epsilon_B[B]}\{1-e^{-2.303(\epsilon_A[A]+\epsilon_B[B])l}\} \quad (2)$$

quantum yield, I_0 is the light intensity, N is Avogadro's number, V is the cell volume, and the other symbols are as defined previously. In the time interval $\Delta t = dt$ where $\Delta A = d[A] = ([A]_{final} = A_f) - ([A]_{initial} = A_i)$, a transcendental equation may be written for A_f as in eq 3. Given A_i and an initial value of Φ and assuming $A_f = A_i$,

$$A_f = A_i - \frac{\Delta t\Phi I_0\epsilon_A([A_i+A_f]/2)\times[1-e^{-2.303l\{\epsilon_A([A_f+A_i]/2)+\epsilon_B(W_0-[A_i+A_f]/2\}}]}{(6.023\times10^{23})V\{\epsilon_A([A_f+A_i]/2)+\epsilon_B(W_0-[A_f+A_i]/2)\}} \quad (3)$$

A_f, the concentration of A after time Δt, may be calculated by the process of successive approximations such that A_f on the left and right sides of eq 3 agree to within a set limit of error. This value of A_f then becomes A_i for the next time interval $\Delta t'$. In this way a theoretical function of [A] vs. time is calculated for a given Φ. Curves are generated for a range of Φ and are compared to the experimental data to determine which Φ best fits the observed behavior using a nonlinear least-squares procedure. All calculations were performed on a PDP 11/45 computer.

3. Instrumentation for Spectral Analysis. Ultraviolet–visible spectra were recorded on Cary 11, 14, and 15 spectrophotometers. A Varian A-60D spectrometer was used for proton NMR spectra. Infrared spectra were obtained using a Perkin-Elmer 421 or 521 spectrometer. All IR spectra of the carbonyl region were recorded on a Beckman IR-4 using the widest spectral expansion.

Liquid-nitrogen temperature emission spectra were obtained with a Spex Flourolog photophosphorimeter modified to accept a quartz Dewar in the sample compartment. The sample holders were 8-mm o.d. Pyrex tubes. All solvents used for glasses were purified and triply distilled.[23]

Results

1. Spectra Studies. Ultraviolet–Visible Electronic Spectra. The monosubstituted derivatives of tungsten hexacarbonyl display three types of electronic spectra. Figure 1 shows representative examples of each type. Nitrogen-donor complexes have an intense band at about 4000 Å (labeled B) with a red shoulder (labeled A). Phosphorus-donor compounds, Figure 1b, show features which are blue shifted relative to the amine materials. A two-band pattern is found on the side of the first intense charge-transfer (~3000 Å) peak. These two peaks are labeled C and D. The remaining complexes all show a low energy set of bands, E and F, of moderate intensity. The energies of each labeled band for all complexes studied have been recorded in Table I.

Emission Spectra. High-resolution, 77 K emission spectra were obtained for all nitrogen- and phosphorus-donor systems. The luminescence maxima always occurred in the 5300-Å

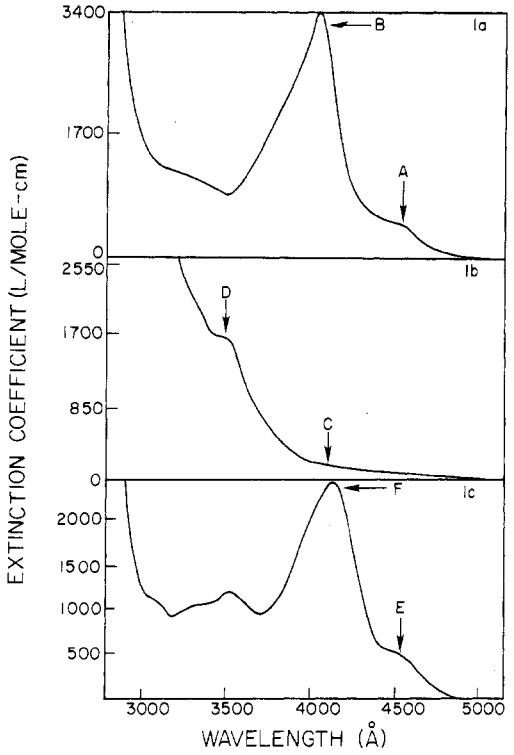

Figure 1. Low-energy absorption features in the room-temperature electronic spectra of: (a) $W(CO)_5(c\text{-}HxNH_2)$ in cyclohexane; (b) $W(CO)_5PPh_3$ in cyclohexane; (c) $W(CO)_5Br^-NEt_4^+$ in THF.

Table I. Energies of Electronic Spectral Features of $W(CO)_5L$ Compounds (Cyclohexane Solvent)

L	Energy of band maximum,[a] $cm^{-1} \times 10^3$	
Nitrogen donors:	Band A	Band B
Acetonitrile	24.1	26.3
NH_3[b]	22.1	24.5
Cyclohexylamine	22.1	24.6
Pyridine	22.4	26.3
Piperidine	22.1	24.5
Phosphorus donors:	Band C	Band D
PPh_3	25.8	28.5
PBr_3	24.4	29.4
PCl_3	25.3	29.2
PH_3	*d*	29.2
$P(n\text{-}Bu)_3$	26.3	28.5
Other ligands:	Band E	Band F
CS	22.5	23.9
Br^-[b]	22.1	24.4
$C(CH_3)(OCH_3)$	22.0[c]	
$C(Ph)(OCH_3)$	19.4[c]	

[a] Band labels keyed to Figure 1. [b] $CHCl_3$ solvent. [c] Lowest energy band in the spectrum. [d] Not resolved.

(18.8×10^3 cm^{-1}) region and appeared to be independent of whether the complex exhibits the absorption spectra of Figure 1a or 1b. The correspondence of the emission energy of $W(CO)_5L$ over a wide range of ligands, L, has been discussed in the literature.[25] The remaining compounds (L = CS, Br^-, and carbene) exhibited no detectable luminescence.

Vibrational Spectra. Carbonyl infrared stretching frequencies of the $W(CO)_5L$ complexes were recorded in cyclohexane. The Cotton–Kraihanzel force factored field approximation[26] was used to calculate the force constants from the three infrared active modes. The most intense band was always assigned to the E vibration resulting in k_1 (trans CO) always being smaller than k_2 (cis CO) consistent with the theoretical assumptions of ref 26. The IR assignments and calculated force constants are tabulated in Table II.

Table II. Infrared Data and Carbonyl Force Constants[a] of $W(CO)_5L$ Compounds (Cyclohexane Used as Solvent)

	Band energies, cm^{-1}			Calcd force constants		
$W(CO)_5L$, L	$A_1^{(1)}$	$A_1^{(2)}$	E	k_1 (trans)	k_2 (cis)	k_i, mdyn/A
Acetonitrile	2077	1926	1944	15.13	15.93	0.34
Cyclohexylamine	2072	1917	1930	15.00	15.75	0.36
Pyridine	2072	1919	1932	15.03	15.77	0.35
Piperidine	2065	1917	1926	15.00	15.67	0.35
PPh_3	2072	1944	1944	15.42	15.90	0.32
PBr_3	2095	1990	1984	16.14	16.46	0.28
PCl_3	2083	1985	1981	16.05	16.36	0.26
PH_3	2084	1956	1956	15.61	16.09	0.32
$P(n\text{-}Bu)_3$	2065	1941	1935	15.38	15.76	0.32
CS	2097	2008	1989	16.45	16.51	0.27
Br^-[b]	2072	1893	1923	14.63	15.68	0.37
$C(CH_3)(OCH_3)$	2073	1961	1938	15.73	15.83	0.34
$C(Ph)(OCH_3)$	2073	1961	1944	15.71	15.90	0.32
CO	1985 T_{1u}			$k = 16.41$[c]		0.29[c]

[a] Calculated using ref 26. [b] KBr pellet. [c] From ref 26.

2. Ligand-Substitution Photochemistry. Nitrogen-Donor Complexes. The nitrogen-donor complexes were irradiated in their lowest energy absorption feature (Figure 1, band A) at 4358 Å in an inert, degassed solvent maintained in a brass block thermostated at 7 ± 2 °C and containing approximately a 1 M concentration of the entering ligand, L′. L′ was either another amine or carbon monoxide.[27] Isosbestic points were observed in the UV–visible spectra of the photolyte when irradiation was carried out to about 25% conversion. Longer irradiation resulted in degradation of these points, probably because of significant formation of higher substitution products. When isosbestic points were found, the photoproduct could be identified from the appearance of features in the UV–visible and infrared spectra attributable to a monosubstituted species $W(CO)_5L'$. At 7 °C, thermal ligand exchange accounted for approximately 5% of the total conversion to product and no correction of the quantum yield was attempted. When L′ = CO the reactions were run at room temperature and no evidence was found of thermal ligand replacement. A photochemical back-reaction of $W(CO)_5L'$ with photogenerated free L to produce $W(CO)_5L$ is suppressed by the high concentration ratios of L′ to $W(CO)_5L$.

In order to obtain quantum yields for carbon monoxide loss from $W(CO)_5L$, L was used as the entering ligand. The quantum yields for production of $W(CO)_4L_2$ were at the limits of detection of the analytical methods employed. The low quantum efficiency of production of disubstituted products, which were always of cis configuration, is consistent with the observation of isosbestic points when $L' \neq L$ or CO.

Table III contains the quantum yields for these systems as well as some data from previous studies. The general pattern found for these complexes is efficient unique ligand photosubstitution and a much lower efficiency carbon monoxide loss reaction resulting in cis products.

Phosphorus-Donor Complexes. Irradiation into the lowest energy spectral feature (band C, Figure 1) at 4050 Å of complexes with phosphorus-donor ligands was carried out at room temperature in a variety of solvents which were chosen for their ability to dissolve the photoproduct. It became immediately obvious that the procedures developed for nitrogen-donor complexes would not work well for the phosphorus donors because of problems with air sensitivity and thermal reactivity. Triphenyl phosphite was used as an entering ligand for $W(CO)_5L$ (L = PPh_3, PCl_3, PH_3, and $P(n\text{-}Bu)_3$) and no isosbestic points were found. This evidence

Table III. Photosubstitution Quantum Yields for Nitrogen-Donor Complexes, $W(CO)_5L$

$W(CO)_5L$, L	Solvent[d]	Entering ligand L′	Wavelength of irradiation, A	Photoproduct	Quantum yield[a]
Acetonitrile	c-Hx[b]	Pyridine	4358	$W(CO)_5(py)$	0.25
Acetonitrile	$CHCl_3$[c]	Acetonitrile	4050	*cis*-$W(CO)_4(AN)_2$	$<10^{-2}$ [e]
NH_3	c-Hx[b,c]	CO	4050	$W(CO)_6$	0.52
NH_3	*i*-Oct[f,g]	1-Pentene	4050	$W(CO)_5$(pentene)	0.66
Cyclohexylamine	c-Hx[b]	Pyridine	4358	$W(CO)_5(py)$	0.26
Piperidine	c-Hx[b]	Pyridine	4358	$W(CO)_5(py)$	0.58
Piperidine	*i*-Oct[f,g]	1-Pentene	4358	$W(CO)_5$(pentene)	0.58
Pyridine	c-Hx[b]	Piperidine	4358	$W(CO)_5$(pip)	0.12
Pyridine	$CHCl_3$[c]	CO	4050	$W(CO)_6$	0.22
Pyridine	c-Hx[b]	Pyridine	4358	*cis*-$W(CO)_4(py)_2$	0.002
Pyridine	*i*-Oct[f,h]	Pyridine	4358	*cis*-$W(CO)_4(py)_2$	0.002

[a] Quantum yield for appearance of photoproduct, error estimated at ±15%. [b] Cyclohexane. [c] 25 °C. [d] All at 7 °C. [e] Lower limit of detection. [f] Isooctane. [g] Reference 8. [h] Reference 7.

Table IV. Photosubstitution Quantum Yields for Phosphorus-Donor Complexes, $W(CO)_5L$[a]

$W(CO)_5L$[b]	Solvent	Entering ligand[b]	Photoproduct	Quantum yields[c]
PPh_3	c-Hx[d]	CO	$W(CO)_6$	0.29
PPh_3 [5×10^{-3}]	$CHCl_3$	PPh_3 [0.1]	*cis*-$W(CO)_4(PPh_3)_2$	0.18
PPh_3 [3×10^{-3}]	$CHCl_3$	PPh_3 [0.1]	*cis*-$W(CO)_4(PPh_3)_2$	0.22
PPh_3 [2×10^{-3}]	$CHCl_3$	PPh_3 [0.1]	*cis*-$W(CO)_4(PPh_3)_2$	0.26
PPh_3 [1×10^{-3}]	$CHCl_3$	PPh_3 [0.1]	*cis*-$W(CO)_4(PPh_3)_2$	0.29
PPh_3 [5×10^{-4}]	$CHCl_3$	PPh_3 [1.0]	*cis*-$W(CO)_4(PPh_3)_2$	0.50
PPh_3 [5×10^{-4}]	$CHCl_3$	PPh_3 [10^{-2}]	*cis*-$W(CO)_4(PPh_3)_2$	0.51
PPh_3 [5×10^{-4}]	THF	PPh_3 [0.1]	*cis*-$W(CO)_4(PPh_3)_2$	0.46
PCl_3	c-Hx[d]	CO	$W(CO)_6$	0.028
PBr_3	c-Hx[d]	CO	$W(CO)_6$	0.22
PH_3	c-Hx[d]	CO	$W(CO)_6$	0.65
$P(n\text{-}Bu)_3$	c-Hx[d]	CO	$W(CO)_6$	0.25

[a] All at 25 °C. [b] Concentration bracketed. [c] Quantum yield for appearance of photoproduct. Estimated error ±15%. [d] Cyclohexane.

was the first to implicate a new mode of photoreactivity for these materials; i.e., carbon monoxide substitution when L′ ≠ L or CO results in formation of mixed ligand higher substitution products, $W(CO)_4LL'$. These disubstituted compounds are known to be photoactive.[28] Secondary photolysis causes the ratio of photoproducts to change as a function of irradiation time and hence prevents observation of isosbestic points. These problems did not occur in the nitrogen-donor studies because the quantum efficiency for CO loss was much lower than in the phosphorus systems.

The quantum yield for unique ligand loss was determined using L′ = CO. Although isosbestic points were not observed, the increase of the T_{1u} IR band of the $W(CO)_6$ photoproduct provided sufficient data for establishing the appearance quantum yield for $W(CO)_6$ for all of the phosphorus-donor complexes which was within experimental error of the disappearance quantum yield when photolysis was carried out to less than 10% conversion. These reactions were carried out in CO-saturated cyclohexane. Table IV contains the quantum yields and experimental conditions. Experiments utilizing L′ ≠ L or CO resulted in several products and accurate quantum yields could not be obtained.

When L = PPh_3, the reaction of $W(CO)_5PPh_3$ (where L′ = L) could be interpreted quantitatively due to the appearance of an isosbestic point in the UV–visible spectrum. Infrared spectroscopy demonstrated that the only photoproduct was *cis*-$W(CO)_4(PPh_3)_2$. All other complexes underwent extensive decomposition under these conditions. Table IV contains data for the PPh_3 systems studied. Although the quantum efficiency for CO loss varies with $W(CO)_5L$ concentration,[29] under all conditions this reaction is much more efficient than the analogous reaction in the nitrogen-donor systems. The above observations show that loss of carbon monoxide is more efficient for all of the phosphorus-donor materials studied than for nitrogen donors. This new photochemical reaction pathway does not proceed at the expense of the unique ligand-substitution reaction which, except for L = PCl_3, is operative at undiminished efficiency compared to the nitrogen donors.

Photolysis of 10^{-2} M solutions of $W(CO)_5PPh_3$ in the presence of 1 equiv of 90 atom % ^{13}CO in sealed tubes with either broad-band or 4050-Å radiation resulted in products with high ^{13}CO enrichments in the equatorial positions after chromatographic separation from $W(CO)_5(^{13}CO)$. In all preparations attempted the ratio of cis to trans enrichment equaled or exceeded the 4:1 statistical ratio.

Remaining Materials. Of the remaining complexes $W(CO)_5L$ (L = CS, Br^-, methylmethoxycarbene, and phenylmethoxycarbene) none demonstrated a quantum yield for photosubstitution larger than about 10^{-2}. Data for these substances are presented in Table V.

Upon irradiation of the carbene complexes in carbon monoxide saturated cyclohexane for several hours, no detectable changes could be found in the spectra of the phytolytes. The upper limit of the yield is assigned as 10^{-2} for carbene photoreplacement. When L′ = PPh_3, $W(CO)_5PPh_3$ was produced thermally.[30] However, no changes in the carbonyl IR consistent with higher substitution products of

Table V. Photosubstitution Quantum Yields for Class 3 Complexes, at 4050 A[a]

$W(CO)_5L$, L	Solvent	Entering ligand L′	Photoproduct	Quantum yield[b]
CS	$CHCl_3$	PPh_3	$W(CO)_5PPh_3$ + $W(CO)_4CS(PPh_3)$	$<10^{-2}$
CS	c-Hx[c]	PPh_3	$W(CO)_5PPh_3$ + $W(CO)_4CS(PPh_3)$	$<10^{-2}$
Methylmethoxycarbene	c-Hx[c]	CO	$W(CO)_6$	$<10^{-2}$
Phenylmethoxycarbene	c-Hx[c]	CO	$W(CO)_6$	$<10^{-2}$
$Br^-(NEt_4^+$ salt)	$CHCl_3$	CO	$W(CO)_6$	1.2×10^{-2}
$Br^-(NEt_4^+$ salt)	$CHCl_3$	Acetonitrile	$W(CO)_4(AN)Br^-$	$<10^{-2}$ [d]

[a] 25 °C. [b] 10^{-2} is the lower limit of detection. [c] Cyclohexane. [d] A thermal reaction produced $W(CO)_5(AN)$; however, there was no evidence of higher substitution products.

the type $W(CO)_4(PPh_3)$(carbene) were observed upon irradiation.

Photolysis of $W(CO)_5CS$ in either $CHCl_3$ or cyclohexane solution with L′ = PPh_3 produces $W(CO)_5PPh_3$ which reaches a limiting value corresponding to about 1% conversion. This probably results from substitution of $W(CO)_6$ impurities in this material. The rate of disappearance of the E vibrational band of $W(CO)_5CS$ in the IR spectra during irradiation was indicative of a quantum yield for ligand replacement of less than 10^{-2}. A recent matrix isolation study of $W(CO)_5CS$ indicated that the major photoproduct resulted from carbon monoxide loss.[31] In solution this reaction occurs with low efficiency and is not comparable to the photochemistry of $W(CO)_6$ as suggested in ref 31.

When $W(CO)_5Br^-$ was irradiated in the presence of CO, a quantum yield of approximately 10^{-2} for Br^- photoreplacement was observed. Use of L′ = acetonitrile resulted in a rapid thermal exchange. However, the UV–visible spectra of the photolytes still showed the isosbestic points of the $W(CO)_5Br^-/W(CO)_5$(AN) pair, thus indicating that carbon monoxide loss is not a significant photosubstitution path.

Discussion

1. Classification of the Photochemical Reactivity. Three reactivity patterns were found for the photosubstitution reactions for monosubstituted derivatives of tungsten hexacarbonyl. These reaction pathways are summarized in eq 4 to 6.

Class 1 reactivity:

$$W(CO)_5A \xrightarrow[+L']{h\nu\,\phi_1} W(CO)_5L' + A \quad (4a)$$

$$W(CO)_5A \xrightarrow[+L']{h\nu\,\phi_2} W(CO)_4AL' + CO \quad (4b)$$

A = acetonitrile, cyclohexylamine, NH_3, $N(n\text{-}Pr)H_2$, piperidine, pyridine; $\phi_1 \simeq 0.5$; $\phi_2 < 10^{-2}$.

Class 2 reactivity:

$$W(CO)_5P \xrightarrow[+L']{h\nu\,\phi_1} W(CO)_5L' + P \quad (5a)$$

$$W(CO)_5P \xrightarrow[+L']{h\nu\,\phi_2} W(CO)_4PL' + CO \quad (5b)$$

P = PPh_3, PBr_3, PCl_3, PH_3, $P(n\text{-}Bu)_3$; $\phi_1 \simeq \phi_2 \simeq 0.3$.

Class 3 reactivity:

$$W(CO)_5C \xrightarrow[+L']{h\nu\,\phi_1} \text{various substitution products} \quad (6)$$

C = methylmethoxycarbene, phenylmethoxycarbene, CS, Br^-; $\phi_1 \leq 10^{-2}$.

For substituted carbonyl complexes in which photodissociation of either a metal–carbonyl carbon or metal–unique ligand bond can occur, these classes represent three of the four possible permutations of product distribution. Class 1 behavior is characterized by highly efficient unique ligand photosubstitution with small carbon monoxide loss. Class 2 demonstrates high reactivity in both metal–carbonyl and metal–unique ligand bonds. Class 3 shows reduced activity in both bond types. The fourth possible classification would consist of reduced unique ligand loss with efficient carbon monoxide substitution. Over the range of materials studied (with the possible exception of L = PCl_3), this pattern has not been observed (vide infra).

The experimental evidence suggests that the primary photochemical process is dissociative in character. The quantum yield for carbon monoxide photosubstitution in $W(CO)_5PPh_3$ is constant over three orders of magnitude of entering ligand concentration (Table IV). Furthermore, the quantum efficiency of CO loss is the same in both $CHCl_3$ and THF within experimental error. In the latter solvent, 12.3 M THF can function as a nucleophile in the initial photochemical step forming the metal–THF adduct. When different entering ligands are used to trap the photoproducts, the quantum yields do not vary[7] indicating that the photoreaction is not sensitive to the nature of the entering ligands. A dissociative photoprocess is consistent with thermal measurements which show that although both associative and dissociative paths exist for ligand replacement in the ground state of analogous molybdenum complexes, only about 5 to 8 kcal/mol of bond formation is involved in the transition state.[32] Due to the net reduction of the metal–ligand bond order in the excited state relative to the ground state (vide infra), the associative process should be of even less importance in photosubstitution.

Although cis disubstituted products were obtained for the reaction in which carbon monoxide substitution was studied in detail, it is not certain that the stereochemistry of the products accurately reflects the position of CO loss in the primary step. The labeling experiments showed that $W(CO)_5PPh_3$ was photochemically enriched in both cis and trans position and that pure trans-labeled material could not be obtained via a photochemical path. Darensbourg has conducted enrichment studies on these and similar materials.[33] His results indicate that class 2 compounds show both cis and trans enrichment while class 1 materials may incorporate *CO stereospecifically into cis positions.[34] Because coordinatively unsaturated intermediates of the type $M(CO)_5$ or $M(CO)_4L$ may undergo rapid thermal rearrangements in their ground states before being scavenged by an incoming ligand to re-form a stable 18-electron system, no definite assignment of the position of CO loss based on the uptake of *CO into various sites of the intermediate can be made.[35] Definite stereochemical conclusions require studies in which a labeled CO is lost from the complex and the quantum efficiency of this process is compared to the overall efficiency for disubstituted product formation.

Equations 7 to 9 account for the observed reactions in the framework of a dissociative photoinitiation. The primary photochemical steps are:

$$W(CO)_5L \xrightarrow{h\nu\,\phi_1} W(CO)_5 + L \quad (7)$$

$$W(CO)_5L \xrightarrow{h\nu\,\phi_2} W(CO)_4L(C_s) + CO \quad (8)$$

$$W(CO)_5L \xrightarrow{h\nu\,\phi_3} W(CO)_4L(C_{4v}) + CO \quad (9)$$

The photochemical classes are a consequence of the relative magnitudes of ϕ_1, ϕ_2, and ϕ_3. For class 1, $\phi_1 > \phi_2 + \phi_3$; for class 2, $\phi_1 \simeq \phi_3 + \phi_2$; and for class 3, $1.0 >> \phi_1$, ϕ_2, or ϕ_3. The coordinatively unsaturated intermediates of reactions 8 and 9 may undergo rearrangement competitively with scavenging by entering ligand. In addition it is possible that the six-coordinate products of the scavenging may also rearrange. Thus mechanistic information may not be drawn from the product stereochemistry.

2. Properties Leading to Class 1 and 2 Photochemistry. Spectroscopic Properties. The low-energy features of the electronic spectra of class 1 and 2 compounds (bands A and B, and bands C and D of Figure 1a and 1b, respectively) have previously been assigned as the formally triplet and singlet components of the ligand field transition $A_1 \rightarrow E$.[3b,6,7] The E orbital label is in agreement with photoelectron spectra (PES) which show that the highest occupied molecular orbital in all of these compounds is metal centered and doubly degenerate, i.e., d_{xz}, d_{yz} of e symmetry.[36] Other PES studies have concluded that the b_2 (d_{xy}) orbital always lies below this set.[37]

Class/Compd	$\bar{k}$ ν(C≡O)[a]	M-C Bond Order[b]		Unique Ligand Type
$W(CO)_6$	16.41	Lowest	↑ Most Photoactive M-C Bonds	Strong π Acceptor; Weak σ Donor
Class 2 cis	16.11			Weak π Acceptor; Strong σ Donor
Class 1 cis	15.78			σ Donor Only
Class 2 trans	15.72			Weak π Acceptor; Strong σ Donor
Class 1 trans	15.04	Highest	↓ Photoinert M-C Bonds	σ Donor Only

Figure 2. Empirical ordering of metal–carbon bonds by carbon–oxygen force constants: (a) average value from Table II in mdyn/Å; (b) ground-state bond order. The relative changes in the excited state bond orders are argued in the text.

Whether the lowest excited E state is derived from the 1-electron $b_2^2e^3a_1^1$ ($^2d_{xy}$, $^2d_{xz}$, $^1d_{yz}$, $^1d_{z^2}$) or the $b_2^2e^3b_1^1$ ($^2d_{xy}$, $^2d_{xz}$, $^1d_{yz}$, $^1d_{x^2-y^2}$) configuration has been a point of controversy in the literature.[38,39] Currently we are investigating the magnetic circular dichroism (MCD) spectra of the materials reported here.[40] Preliminary results for $W(CO)_5Br^-$ indicate that the lowest energy excited state arises from population of a d_{z^2} orbital, i.e., $Br_{\pi^*} \rightarrow d_{z^2}$ (vide infra), as evidenced by a positive Faraday A term in analogy with the MCD analysis of isoelectronic $Mn(CO)_5Br$.[41] $W(CO)_5PPh_3$ shows two oppositely signed features on the red shoulder of the first charge-transfer band corresponding to bands C and D of Figure 1b which may be assigned to the two ^3E states arising from T_{1g} and T_{2g} in O_h symmetry.

The proximity of the two E states in $W(CO)_5PPh_3$ leads to the conclusion that they are highly mixed by configuration interaction (CI). A CI eigenfunction for the lowest excited ligand field state may be written as in eq 10[42] where λ is a

$$\Phi_E = \frac{1}{(1+\lambda^2)^{1/2}}\left[\left(\frac{3^{1/2}+\lambda}{2}\right)(^2d_{xy}, {}^2d_{xz}, {}^1d_{yz}, {}^1d_{z^2}) + \left(\frac{1-3^{1/2}\lambda}{2}\right)(d_{xy}, {}^2d_{xz}, {}^1d_{yz}, {}^1d_{x^2-y^2})\right] \quad (10)$$

mixing parameter defining the amount of d_{z^2} character in this state. A value of λ which provides the lowest E state with more d_{z^2} than $d_{x^2-y^2}$ character is required by the MCD results.

Bonding Properties. Trends in the metal–carbonyl carbon bond order can be estimated from vibrational analyses and molecular orbital theory. Both methods reveal a distinction between class 1 and 2 compounds. The strength of the metal–carbon bonds may be crudely estimated from the ν(CO) force constants k. Because both the σ donating and π accepting orbitals of carbon monoxide are antibonding with respect to the carbon–oxygen bond,[43] a large value of k is indicative of a weaker metal–carbon bond in the ground state.[9] The average values of k from Table II for the various types of carbonyl groups in class 1 and 2 compounds, ordered in terms of the expected metal–carbon bond strength, are shown in Figure 2. The same qualitative ordering of metal–carbon bond strength is expected in the excited state because depopulation of the π bonding d_{xz}, d_{yz} orbitals should effect trans carbonyl groups twice as much as cis carbonyls. In the excited state, the class 1 cis and class 2 trans bonds are too close to differentiate. The gap between class 1 trans and the other bond types in Figure 2 empirically defines those metal–carbon bonds susceptible to photosubstitution.

Simplified molecular orbital considerations support the force constant arguments and suggest origins of the class 1 and 2 photopathways. The energies of the highest occupied molecular orbitals (HOMO) for class 1 compounds (average value of 7.56 eV) and $W(CO)_6$ (8.56 eV) have been determined in PES studies.[36,37,44] PES of the analogous $Cr(CO)_5L$ show the energies of the HOMO's of phosphorus-donor derivatives to lie between nitrogen-donor HOMO's and those of $Cr(CO)_6$.[36] This suggests that the relative ordering of the average metal–carbon bond strengths of Figure 2 arises from a ligand inductive effect.[45] The energies of the HOMO have been correlated with the pK_A of simple amines to support this argument.[46] It is expected that the charge induced on the metal decreases in the order class 1 > class 2 > CO in the $W(CO)_6$ limit. The greater the electron density on the central metal, the greater the π back-bonding and the stronger the metal–carbon bonds. Hence, it is the ability of the unique ligand to induce charge on the metal and selectively strengthen metal–carbonyl carbon bonds that underlies the various modes of photochemical CO loss reactions.

Unique Ligand vs. Carbonyl Photolabilization. As has been previously established, the effect of population of the lowest excited state in class 1 or 2 compounds is to cause anisotropic bond weakening by depopulation of π bonding d_{xz}, d_{yz} orbitals and population of the σ antibonding CI orbital which is localized along the unique, z, axis. The unique ligands of both classes are strong σ donors and a major increase in σ antibonding along their z axis will substantially weaken the metal–unique ligand bond and lead to a high quantum efficiency for reaction 7.

In order to labilize a metal–carbonyl carbon bond, that bond must both receive a large σ^* population in the excited state and have a low initial metal–carbon bond order, i.e., it must lie above the empirical dividing line of Figure 2. In class 1 systems the orbital which is populated in the excited state is principally axially directed. However, because the class 1 trans CO has the highest metal–carbon bond order, loss of trans CO (eq 9) proceeds with very low quantum efficiency. Although class 1 cis CO's lie above the empirical limit in Table II, the amount of equatorial σ^* population in the excited state is low and reaction 8 occurs at reduced efficiency. Thus, the total quantum efficiency of CO loss in class 1 materials is low. In contrast, class 2 compounds have a higher degree of CI mixing of the d_{z^2} and $d_{x^2-y^2}$ orbitals in the excited state and thus have a less anisotropic σ^* population than that of the class 1 materials. Because both cis and trans CO lie above the empirical limit of Table II, the total efficiency of reactions 8 and 9 should be large. Note that in $W(CO)_6$, where the σ^* population is isotropic and all metal–carbon bonds lie above the photoactive threshold of Figure 2, carbonyl photosubstitution occurs with unit quantum efficiency.[2]

3. Excited States Leading to Class 3 Behavior. The reduced quantum efficiency of photosubstitution shown by class 3 compounds when irradiated in their lowest energy absorption band is a consequence of the ligand-to-metal charge transfer (LTMCT), metal-to-ligand (MTLCT), or ligand-localized nature of the lowest excited state. The one-electron orbital diagrams accounting for the charge-transfer assignments are shown in Figure 3. For $W(CO)_5CS$ the lowest excited state is assigned as MTLCT as the π^* orbitals of CS are 1.8 eV (14.5×10^3 cm^{-1}) lower in energy than those of CO.[47] The first MTLCT state in $W(CO)_6$ occurs at 34.6×10^3 cm^{-1} [48] and a lowering of the ligand π^* energy should result in a decrease in the energy of this state to a position below the ligand field states as shown in Figure 3. Theoretical calculations on $Cr(CO)_5CS$ and PES studies of both $W(CO)_5CS$ and $Cr(CO)_5CS$ indicate that the HOMO is very close in energy to that of $W(CO)_6$ and the lowest energy one-electron transition is best assigned as population of a low lying CS π^* orbital rather than either the d_{z^2} or $d_{x^2-y^2}$ metal levels.[37] PES of $Mn(CO)_5Br$, isoelectronic with $W(CO)_5Br^-$, show the HOMO to be 80% Br pπ in character.[44] A LTMCT state is therefore implicated for the latter compound as the MCD spectra of both the Mn and W materials are very similar.[40] For the carbene complexes, the lowest excited state of the analogous chromium complexes has been assigned as a ligand-centered $\pi \rightarrow \pi^*$ transition.[49] A recent PES study of these

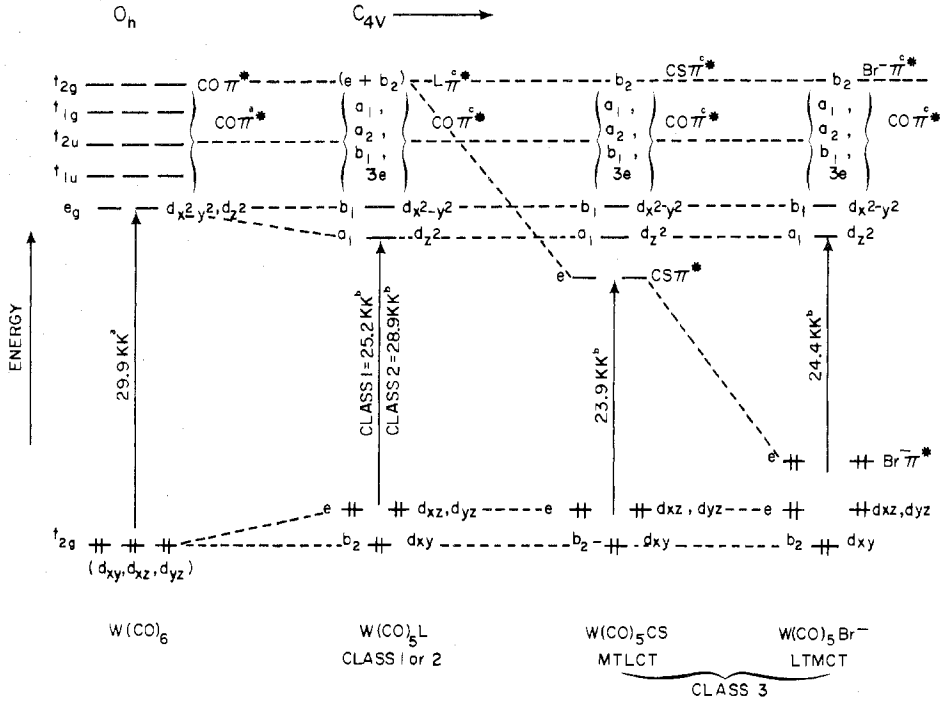

Figure 3. Qualitative molecular orbital scheme for $W(CO)_5L$ compounds: (a) energy from ref 47; (b) energy from bands B, D, and F of Table II; (c) relative energies of these orbitals are uncertain.

chromium materials shows the HOMO's to be Cr 3d in character,[50] implicating a MTLCT state as lowest in energy rather than the $\pi \rightarrow \pi^*$ interligand state. In all cases of class 3 behavior, the lowest excited state is significantly different from the photoactive d–d state of class 1 and 2 compounds. The reduced photosubstitution activity of MTLCT states in tungsten carbonyls has been demonstrated recently.[8] This low efficiency for photosubstitution may now be extended to LTMCT and perhaps intraligand states in the above compounds.

From the viewpoint of a bonding model, this photosubstitution inactivity suggests that σ^* population must be accompanied by π bonding decreases in order to achieve efficient photosubstitution. Alternatively, the lack of emission from these materials points to an increased rate of nonradiative deactivation of their excited states. On the basis of the similarity of the oscillator strengths of the absorption bands there is no reason to expect that in low temperature glasses the rate of luminescence from class 1, 2, or 3 compounds should be very different. A large nonradiative rate constant in class 3 materials, which could reduce the luminescence efficiency at low temperature, might carry over to room-temperature solutions resulting in a reduction of the photochemical substitution quantum yield. It is not clear why the nonradiative rate constant should be larger for class 3 compounds than those for classes 1 and 2.

That the fourth possible photochemical path has not been observed, i.e., efficient carbon monoxide loss with little unique ligand substitution, is consistent with the foregoing arguments. Reasoning from the bonding model, a class 4 complex would require a unique ligand which is a stronger π acceptor than CO and of equal or reduced σ donor strength. If such a ligand exists, however, the increased π interaction would result in a lowering of the ligand π^* states which has been seen to result in the class 3 MTLCT state which is inefficient for any photosubstitution. It is interesting to note that the observed photoreaction of $W(CO)_5CS$, the complex most approaching the necessary conditions for class 4 behavior, is predominantly inefficient loss of carbon monoxide consistent with increased positive character on the tungsten and hence weakening of the metal–carbonyl carbon bonds in the MTLCT state. This explanation is supported by the ν(CO) force constants in Table II. That efficient carbon monoxide photosubstitution does not occur in this material may result either from the lack of increased σ^* population in the charge-transfer state or from increased nonradiative deactivation from this state.

Acknowledgment. J.I.Z. gratefully acknowledges the receipt of a Camille and Henry Dreyfus Teacher-Scholar Award, 1974–1979.

Registry No. $W(CO)_5(AN)$, 15096-68-1; $W(CO)_5NH_3$, 15133-64-9; $W(CO)_5$(c-HxNH$_2$), 16969-84-9; $W(CO)_5P(n\text{-Bu})_3$, 17000-19-0; $W(CO)_5$(pip), 31082-68-5; $W(CO)_5$(py), 14586-49-3; $W(CO)_5Br^-NEt_4^+$, 14780-94-0; $W(CO)_5PPh_3$, 15444-65-2; $W(CO)_5$(methylmethoxycarbene), 15975-98-1; $W(CO)_5$(phenylmethoxycarbene), 25879-49-6; $W(CO)_5PBr_3$, 22466-08-6; $W(CO)_5PCl_3$, 21223-85-8; $W(CO)_5PH_3$, 23807-48-9; $W(CO)_5CS$, 50358-92-4; (Ac)$W(CO)_5^-NMe_4^+$, 15975-95-8; (Bz)$W(CO)_5^-NMe_4^+$, 15975-92-5; *cis*-$W(CO)_4(AN)_2$, 29890-10-6; $W(CO)_6$, 14040-11-0; $W(CO)_5$(pentene), 53261-74-8; *cis*-$W(CO)_4(py)_2$, 16743-01-4; *cis*-$W(CO)_4(PPh_3)_2$, 38800-77-0; $W(CO)_4CS(PPh_3)$, 64281-55-6; $W(CO)_4(AN)Br^-$, 64215-89-0.

References and Notes

(1) W. Strohmeier and D. Von Hobe, *Chem. Ber.*, **94**, 761 (1961).
(2) W. Strohmeier, *Angew. Chem., Int. Ed. Engl.*, **3**, 730 (1964).
(3) (a) V. Balzani and V. Carassiti, "Photochemistry of Coordination Compounds", Academic Press, New York, N.Y., 1970, pp 323–356; (b) A. W. Adamson and P. D. Fleischauer, "Concepts of Inorganic Photochemistry", Wiley, New York, N.Y., 1975, Chapter 6, p 269.
(4) M. Wrighton, *Chem. Rev.*, **74**, 401 (1974).
(5) W. Strohmeier and D. Von Hobe, *Chem. Ber.*, **94**, 2031 (1961).
(6) M. Wrighton, G. S. Hammond, and H. B. Gray, *Mol. Photochem.*, **5**, 179 (1973).
(7) M. Wrighton, *Inorg. Chem.*, **13**, 905, (1974).
(8) M. Wrighton, *J. Am. Chem. Soc.*, **98**, 4105 (1976).
(9) L. E. Orgel, *Inorg. Chem.*, **1**, 25 (1962).
(10) W. Strohmeier and G. Schonauer, *Chem. Ber.*, **94**, 1346, (1961).
(11) R. J. Angelici and M. D. Malone, *Inorg. Chem.*, **6**, 1731 (1967).
(12) R. J. Dennenberg and D. J. Darensbourg, *Inorg. Chem.*, **11**, 72 (1972).
(13) B. L. Ross, J. G. Grasselli, W. M. Ritchey, and H. D. Kaesz, *Inorg. Chem.*, **2**, 1023 (1963).
(14) R. A. Brown and G. R. Dobson, *Inorg. Chim. Acta*, **6**, 65 (1972).
(15) E. W. Abel, I. S. Butler, and J. G. Reid, *J. Chem. Soc.*, 2068 (1963).
(16) T. A. McGee, C. N. Matthews, T. S. Wang, and J. H. Wotiz, *J. Am. Chem. Soc.*, **83**, 3200 (1961).
(17) E. O. Fischer and A. Maasbol, *Chem. Ber.*, **100**, 2445 (1967).

(18) E. O. Fischer and L. Knauss, *Chem. Ber.*, **102**, 223 (1969).
(19) R. Poilblanc and M. Bigorgne, *Bull. Soc. Chim. Fr.*, **29**, 1301 (1962).
(20) J. A. Connor, E. M. Jones, and G. K. McEwen, *J. Organomet. Chem.*, **43**, 357 (1972).
(21) E. O. Fischer, E. Louis, and R. J. J. Schneider, *Angew. Chem., Int. Ed. Engl.*, **7**, 136 (1968).
(22) B. D. Dombek and R. J. Angelici, *J. Am. Chem. Soc.*, **95**, 7516 (1973).
(23) W. L. Jolly, "The Synthesis and Characterization of Inorganic Compounds", Prentice-Hall, Englewood Cliffs, N.J., 1970, p 114.
(24) (a) J. G. Calvert and J. N. Pitts, "Photochemistry", Wiley, New York, N.Y., 1966, p 783; (b) *ibid.*, p 737.
(25) (a) M. Wrighton, G. S. Hammond, and H. B. Gray, *J. Am. Chem. Soc.*, **93**, 4336 (1971); (b) M. Wrighton, G. S. Hammond, and H. B. Gray, *Inorg. Chem.*, **11**, 3122 (1972).
(26) F. A. Cotton and C. S. Kraihanzel, *J. Am. Chem. Soc.*, **84**, 4432 (1962).
(27) The concentration of CO in cyclohexane at saturation is 0.016 M.
(28) R. Mathieu and R. Poilblanc, *Inorg. Chem.*, **11**, 1858 (1972).
(29) The quantum yield for formation of *cis*-$W(CO)_4(PPh_3)_2$ varies inversely as a function of $W(CO)_5PPh_3$ concentration. We have evidence that in the absence of an entering ligand the following reaction occurs: $2W(CO)_5PPh_3 + h\nu \rightarrow W(CO)_6 + cis\text{-}W(CO)_4(PPh_3)_2$. The concentration dependence of the quantum yield may be a result of this reaction. Further studies are in progress.
(30) E. O. Fischer, E. Louis, and W. Bathelt, *J. Organomet. Chem.*, **20**, 147 (1969).
(31) M. Poliakoff, *Inorg. Chem.*, **15**, 2022 (1976).
(32) W. D. Covey and T. L. Brown, *Inorg. Chem.*, **12**, 2820 (1973).
(33) G. Schwenzer, M. Y. Darensbourg, and D. J. Darensbourg, *Inorg. Chem.*, **11**, 1967 (1972).
(34) D. J. Darensbourg, personal communication.
(35) (a) J. D. Atwood and T. L. Brown, *J. Am. Chem. Soc.*, **98**, 3155 (1976); (b) *ibid.*, **98**, 3160 (1976).
(36) B. R. Higginson, D. R. Lloyd, J. A. Connor, and J. H. Hillier, *J. Chem. Soc., Faraday Trans. 2*, **70**, 1418 (1974).
(37) D. L. Lichtenberger and R. F. Fenske, *Inorg. Chem.*, **15**, 2015 (1976).
(38) M. Wrighton, D. L. Morse, H. B. Gray, and D. K. Ottesen, *J. Am. Chem. Soc.*, **98**, 1111 (1976).
(39) F. A. Cotton, W. T. Edwards, F. C. Rauch, M. A. Graham, R. N. Perutz, and J. J. Turner, *J. Coord. Chem.*, **2**, 247 (1973).
(40) This MCD study is in collaboration with Professor A. F. Schreiner, North Carolina State University, Raleigh, N.C.
(41) R. M. E. Vliek and P. J. Zandstra, *Chem. Phys. Lett.*, **31**, 487 (1975).
(42) M. J. Incorvia and J. I. Zink, *Inorg. Chem.*, **13**, 2489 (1974).
(43) R. F. Fenske, *Pure Appl. Chem.*, **27**, 61 (1971).
(44) D. L. Lichtenberger, A. C. Sarapu, and R. F. Fenske, *Inorg. Chem.*, **12**, 702 (1973).
(45) The HOMO's of $W(CO)_6$ lie lower in energy than those of class 1 compounds due to a higher positive change on the metal in the former case when the unique ligand, CO, is not a strong σ donor and can accept electron density from the metal into ligand π^* orbitals. Phosphorus-donor complexes, which also can accept electron density from the metal due to π interactions, have HOMO energies intermediate between the class 1, strong σ donors, and the hexacarbonyl.
(46) M. A. M. Meester, R. C. J. Vriends, D. J. Stufkens, and K. Vrieze, *Inorg. Chim. Acta*, **19**, 95 (1976).
(47) W. G. Richards, *Trans. Faraday Soc.*, **63**, 257 (1967).
(48) N. A. Beach and H. B. Gray, *J. Am. Chem. Soc.*, **90**, 5713 (1968).
(49) E. O. Fischer, C. G. Kreiter, H. J. Kollmeier, J. Müller, and R. D. Fischer, *J. Organomet. Chem.*, **28**, 237 (1971).
(50) T. F. Block and R. F. Fenske, *J. Am. Chem. Soc.*, **99**, 4321 (1977).

Contribution No. 3719 from the Department of Chemistry, University of California, Los Angeles, California 90024

Photolabilization of Ligands Including Carbon Monoxide from Low-Spin d^6 Iron(II) Macrocyclic Complexes

MICHAEL J. INCORVIA and JEFFREY I. ZINK*

Received October 1, 1976 AIC607229

The photochemistry of low-spin d^6 $[Fe(TIM)(X)(Y)](PF_6)_2$ (TIM = 2,3,9,10-tetramethyl-1,4,8,11-tetraazacyclotetradeca-1,3,8,10-tetraene; X and Y = MeCN, CO, imidazole, and triethyl phosphite) is studied in various organic solvents. The electronic absorption spectra contain an intense metal-to-ligand charge-transfer band in the visible region characteristic of the Fe^{2+}–α-diimine moiety. The energy of this band varies with the π interaction between the metal and the axial ligands. The photochemistry of $[Fe(TIM)CH_3CN(CO)](PF_6)_2$ shows two reaction modes: loss of CH_3CN in acetone and loss of CO in acetonitrile. The bis(triethyl phosphite) complex undergoes photosolvation when the MTLCT band is irradiated in pyridine to form $[Fe(TIM)(py)_2]^{2+}$. The bis(imidazole) complex is photoinert. The photoreactivity of the Fe(II)–TIM complexes is discussed in terms of ligand field and charge-transfer excited-state origins. The temperature dependence of the quantum yield for the photosolvation of the bis(triethyl phosphite) complex in pyridine is examined. The quantum yield varies from 0.0018 at 10 °C to 0.0038 at 40 °C. The activation energy for the photoreaction is 4.1 kcal/mol.

Introduction

Six-coordinate low-spin d^6 complexes of the first, second, and third transition series constitute the largest category of photochemically studied coordination complexes.[1,2] With the use of strong-field ligands, Fe(II) can form low-spin six-coordinate complexes.[3] To date, most of the photochemical studies of Fe(II) complexes, including those of Fe(II) macrocyclic complexes,[4] have dealt with their photoredox properties.[1,5]

Six-coordinate Fe(II) complexes containing the quadradentate, macrocyclic ligand TIM (TIM = 2,3,9,10-tetramethyl-1,4,8,11-tetraazacyclotetradeca-1,3,8,10-tetraene), first synthesized by Rose et al.,[6] were chosen in order to study the ligand substitution photochemistry of low-spin Fe(II). Since this strong-field macrocyclic ligand only adopts a planar configuration in the metal's coordination sphere,[6,7] a variety of trans-disubstituted low-spin complexes can be prepared. Consequently, their photochemical properties can be examined and compared to those of other low-spin d^6 metal systems.[8]

In addition to providing a number of low-spin d^6 iron compounds, the Fe(II)–TIM system has two other important characteristics. First, it binds carbon monoxide. Photochemical studies of carbonyl complexes of iron macrocyclic systems may provide a bridge between the photochemistry of the zerovalent metal carbonyls and the classical ionic "Werner" complexes. In addition, these ionic carbonyl complexes may act as model systems for the photoactivity of carbon monoxide on myoglobin and hemoglobin.[5,9-12] Second, the most intense spectroscopic feature in the visible electronic absorption spectrum is an iron to TIM charge-transfer band. These complexes may help to further elucidate the effect of the CT excited state on ligand photosubstitution reactions.

Experimental Section

Synthesis. **$[Fe(TIM)(CH_3CN)_2](PF_6)_2$**, **$[Fe(TIM)(im)_2](PF_6)_2$**, and **$[Fe(TIM)CH_3CN(CO)](PF_6)_2$** were prepared according to the methods of Baldwin et al.[6]

$[Fe(TIM)(P(OEt)_3)_2](PF_6)_2$. The bis(acetonitrile) complex (0.5 g) was dissolved in 10 mL of acetonitrile and filtered. Triethyl phosphite (2.5 mL) was added to the filtrate. In about 45 s, the solution turned from red to pink-purple. The solution was rotovapped at room temperature until crystals formed and then was filtered. The crystals were washed with diethyl ether and recrystallized from acetone and diethyl ether; yield 80%. Anal. Calcd for $FeC_{26}H_{54}F_{12}N_4O_6P_4$: C, 33.7; H, 5.8. Found: C, 33.9; H, 5.8.

$[Fe(TIM)(NH_3)_2](PF_6)_2$. Dry ammonia gas was vigorously bubbled through a filtered, saturated solution of the bis(acetonitrile) complex in CH_2Cl_2 until the solution was reduced to half its original volume.